A robust separable image denoising based on relative intersection of confidence intervals rule

Damir Seršić and Ana Sović
Faculty of Electrical Engineering and Computing
University of Zagreb
Croatia
damir.sersic@fer.hr, ana.sovic@fer.hr

***Abstract*—Many microscopy images, or 3D depth maps can be represented using piecewise constant models. They usually contain noise due to sensor imperfectness. In this paper, an improved separable denoising method based on the relative intersection of confidence intervals rule is proposed. The method uses median averaging and is robust to outliers and different noise distributions. It over-performs competitive methods in the sense of edge preservation.**

Keywords—Intersection of confidence intervals; Image denoising; Median; Adaptive filters

I. Introduction

Real-world images usually contain noise (especially in dark areas) due to imperfectness or worth of sensors. Sometimes it is very important to reduce noise, e.g. for astronomy [1], microscopy [2], seismology [3], in medicine, where post-processing methods are more acceptable than higher radiation doses [4].

Wiener filtering is a traditional approach to denoising [5]. Wavelet transform shows good performance, especially for non-stationary images with a piecewise polynomial structure of signals and a non-predictable structure of noise [6][7][8]. If the image has piece-wise constant parts, better approaches are the shape adaptive DCT [9], block-matching and 3D filtering algorithm [10] or intersection of confidence intervals (ICI) rule accompanied with local polynomial approximation [11].

In this paper, we use a robust median based technique for enhancement of the known ICI denoising method.

II. Intersection of Confidence Intervals

Let input signal $x(n)$ be corrupted by additive zero mean Gaussian noise $w(n)$. Noise samples are assumed to be independent and identically distributed random variables $\mathcal{N}(0, \sigma_w^2)$:

$$y(n) = x(n) + w(n). \tag{1}$$

Our goal is to find a good estimate $\bar{x}(n)$ of the input signal that accurately restores smooth regions and preserves edges in the same time. Assumption is that the input signal is piecewise constant, so we use zero order estimation on adaptive window length. To obtain the length, we use intersection of confidence intervals (ICI) rule, which chooses filters with short support near edges and long support otherwise.

In one dimensional application of the ICI rule, we increase window length h_k until we reach the optimal size h^* at each observed sample n. Confidence interval is defined for each sample n and for every window length h_k:

$$D_k(n) = \left[\bar{x}_{h_k}(n) - \Gamma \cdot \sigma_{h_k}(n), \bar{x}_{h_k}(n) + \Gamma \cdot \sigma_{h_k}(n)\right], \tag{2}$$

where Γ is a threshold parameter that defines the confidence interval width and $\sigma_{h_k}(n) = \sigma_w / \sqrt{h_k}$ is the deviation of the signal sample estimate [12]. The smallest upper and the largest lower confidence interval limits on observed interval are:

$$\begin{aligned} \overline{L}_k(n) &= \max_{i=1,\dots,k} \left(\bar{x}_{h_i}(n) - \Gamma \cdot \sigma_{h_i}(n)\right), \\ \underline{U}_k(n) &= \min_{i=1,\dots,k} \left(\bar{x}_{h_i}(n) - \Gamma \cdot \sigma_{h_i}(n)\right). \end{aligned} \tag{3}$$

Chosen window length h^+ is the largest window length for which the ICI condition

$$\overline{L}_k(n) \leq \underline{U}_k(n) \tag{4}$$

is satisfied. The same rule must be repeated for every sample of $y(n)$.

Typically, we get a slightly too large window lengths using the ICI rule. A good improvement is a relative intersection of confidence intervals rule (RICI) [13][14]. The method is based on ratio of cumulative confidence interval lengths and the size of the current confidence interval:

$$R_k = \frac{\underline{U}_k(n) - \overline{L}_k(n)}{2\Gamma\sigma_{h_k}}. \tag{5}$$

The chosen window length is the smallest $h^+ = h_k$ for which is satisfied:

$$R_k < r_c, \tag{6}$$

where r_c is a preset threshold parameter. The RICI criterion is usually applied as an additional criterion to the ICI rule.

Using all included samples, with respect to window length h^+, average value on the interval is calculated as:

$$\bar{x}_{h^+}(n) = \text{mean}\,\{y(n), \dots, y(n + h^+(n) - 2), y(n + h^+(n) - 1)\}. \tag{7}$$

In asymptotical sense $(h^+ \to \infty)$ and if the noise distribution is arbitrary, but symmetrical, mean can be replaced by median:

$$\bar{x}_{h^+}(n) = \text{median}\,\{y(n), \dots, y(n + h^+(n) - 2), y(n + h^+(n) - 1)\}. \tag{8}$$

Such a replacement is less sensitive to choice of Γ and r_c, and gives more accurate results for almost any noise distribution. Furthermore, outliers in the signal will almost have no influence on the estimation, thus the estimation is more robust. The edges of the signal will be perfectly restored [15]. We introduce the abbreviations MICI (median intersection on confidence interval) and MRICI (median relative ICI).

III. Image Denoising Algorithm

Zero mean Gaussian noise $w(n,m)$, $\mathcal{N}(0, \sigma_w^2)$, is added to the input image $x(n,m)$:

$$y(n,m) = x(n,m) + w(n,m). \tag{9}$$

A good method for image denoising is described in [16]. We propose using the same algorithm, but with replacing mean averaging with median averaging to get more robust results. The algorithm consists of three stages:

1. For each pixel $y(n,m)$ observe its row. Find the widest window length on the left side $h_{rcL}^+(n,m)$ and on the right side $h_{rcR}^+(n,m)$ from the observed pixel using the ICI or the RICI rule. First letter in an index, r, denotes that the rows are observed first, the second letter, c, means that the columns are observed next, and the third letter symbolizes: L left from the pixel and R right from the pixel. Join all pixels on the intervals and use median:

$$\begin{aligned}\bar{x}_r(n,m) = \text{median}\,\{&y(n, m - h_{rcL}^+(n,m) + 1),\\ &y(n, m - h_{rcL}^+(n,m) + 2), \dots,\\ &y(n,m), \dots,\\ &y(n, m + h_{rcR}^+(n,m) - 2),\\ &y(n, m + h_{rcR}^+(n,m) - 1)\}.\end{aligned} \tag{10}$$

   Now, observe each column of the $\bar{x}_r(n,m)$. Find the widest window length on upper side $h_{rcU}^+(n,m)$ and down side $h_{rcD}^+(n,m)$ from the observed pixel. The third letter symbolizes: U up from the pixel and D down from the pixel. Join the intervals and use median:

$$\begin{aligned}\bar{x}_{rc}(n,m) = \text{median}\,\{&\bar{x}_r(n - h_{rcU}^+(n,m) + 1, m),\\ &\bar{x}_r(n - h_{rcU}^+(n,m) + 2, m), \dots,\\ &\bar{x}_r(n,m), \dots,\\ &\bar{x}_r(n + h_{rcD}^+(n,m) - 2, m),\\ &\bar{x}_r(n + h_{rcD}^+(n,m) - 1, m)\}.\end{aligned} \tag{11}$$

2. Now, do the reverse procedure. At the beginning, observe the column for each pixel $y(n,m)$ and find the widest window length up side $h_{crU}^+(n,m)$ and down side $h_{crD}^+(n,m)$. First letter in index, c, denotes that the columns are observed first, the second letter, r, means that the rows are observed next. Calculate estimation $\bar{x}_c(n,m)$ from pixels in the observed interval:

$$\begin{aligned}\bar{x}_c(n,m) = \text{median}\,\{&y(n - h_{crU}^+(n,m) + 1, m),\\ &y(n - h_{crU}^+(n,m) + 2, m), \dots,\\ &y(n,m), \dots,\\ &y(n + h_{crD}^+(n,m) - 2, m),\\ &y(n + h_{crD}^+(n,m) - 1, m)\}.\end{aligned} \tag{12}$$

   Then, observe each row of the $\bar{x}_c(n,m)$. Find the widest window length on the left side $h_{crL}^+(n,m)$ and on the right side $h_{crR}^+(n,m)$. Calculate estimation $\bar{x}_{cr}(n,m)$ using median:

$$\begin{aligned}\bar{x}_{cr}(n,m) = \text{median}\,\{&\bar{x}_c(n, m - h_{crL}^+(n,m) + 1),\\ &\bar{x}_c(n, m - h_{crL}^+(n,m) + 2), \dots,\\ &\bar{x}_c(n,m), \dots,\\ &\bar{x}_c(n, m + h_{crR}^+(n,m) - 2),\\ &\bar{x}_c(n, m + h_{crR}^+(n,m) - 1)\}.\end{aligned} \tag{13}$$

3. Combine estimated images $\bar{x}_{rc}(n,m)$ and $\bar{x}_{cr}(n,m)$ to the final denoised result. The simplest way is averaging the two estimates:

$$\bar{x}(n,m) = \big(\bar{x}_{rc}(n,m) + \bar{x}_{cr}(n,m)\big)/2. \tag{14}$$

   We denote it as MRICI method with fixed weights. More accurate way is to take weighting factors that depend on reliability of each estimate (MRICI method with the variable weights) [12][16]:

$$\omega_{rc}(n,m) = h^+_{rcL}(n,m) + h^+_{rcR}(n,m) + h^+_{rcU}(n,m) + h^+_{rcD}(n,m),$$

$$\omega_{cr}(n,m) = h^+_{crL}(n,m) + h^+_{crR}(n,m) + h^+_{crU}(n,m) + h^+_{crD}(n,m), \quad (15)$$

$$\bar{x}(n,m) = \frac{\omega_{rc}(n,m)\cdot\bar{x}_{rc}(n,m) + \omega_{cr}(n,m)\cdot\bar{x}_{cr}(n,m)}{\omega_{rc}(n,m) + \omega_{cr}(n,m)}.$$

Proposed method characterizes edge preservation, which is an important feature in the image denoising. Final image is less sensitive to statistical deviations (e.g. outliers) in the image and to sudden changes in the neighboring pixel values. Resulting image has less oscillation near edges. Therefore, it is sharper than when achieved using comparable methods.

Simulation results of the proposed method are presented in the following chapter.

IV. SIMULATION RESULTS

The example is 64x64 pixels test image. It contains gray scale blocks (Fig. 1(a)) and additive zero mean Gaussian noise $\sigma_w = 10$ (Fig. 1(b)). We performed separable image denoising method based on the intersection of confidence intervals rule using mean and a threshold parameter $\Gamma = 4.4$. Final estimated image is calculated using fixed and variable weights (Fig. 1(e) and (f), respectively). Artifacts of separable approach are clearly visible; rows and columns are outstretched. If we replace mean by median inside the ICI rule, we get Fig. 1(g) and (h). The rows and columns are less outstretched, but the edges between different gray shades are not perfectly restored. Fig. 1(i) and (j) shows the estimate calculated using fixed and variable weights and mean based RICI method $\Gamma = 4.4$ and $r_c = 0.85$. The best results are achieved when mean is replaced by median (Fig. 1(k) and (l)). Edges are almost completely preserved and true pixel values are accurately restored.

We compare our results with the anisotropic LPA-ICI, $\Gamma = 1.05$ [17] and non-decimated Haar wavelets (hard threshold $3.5\sigma_w$, 4 decomposition levels) as shown in Fig. 1(c) and (d). In both cases, visual results are worse than in any of the proposed methods. Background is not smooth, and the edges are not sharp.

In Fig. 2(a),(f) the same test image is presented, but with different noise distributions: Laplacian and binomial. Both noisy images are denoised using the anisotropic LPA-ICI method ((b), (g)), undecimated Haar wavelet transform ((c),(h)), mean and median RICI with the fixed weights ((d)-(e), (i)-(j)). In the binomial noise case, the MRICI gives an almost perfectly reconstructed image, while the RICI solution is biased – it gives wrong gray shade level.

Fig. 3 shows PSNR-s for mentioned methods (LPA-ICI, undecimated Haar wavelet transform, separable mean RICI and proposed separable median RICI (MRICI) with fixed weights) for additive Gaussian, Laplacian and binomial noise for noise deviation range of $\sigma_w \in [0,100]$. Separable RICI method results in better PSNR-s for smaller σ_w. Undecimated Haar wavelet and anisotropic LPA-ICI methods show the best results for high levels of the noise. The MRICI outperforms the mean RICI for the lower level of the noise, especially for the additive binomial noise.

In TABLE I. peak signal to noise ratios are compared for the same test image and for three noise distributions: Gaussian, Laplacian and binomial, 30 realizations of each. All noise distributions are zero mean and have $\sigma_w = 10$. In all cases, the new proposed methods show the best PSNR results.

V. CONCLUSION

In this paper we have proposed two novel methods for image denoising which are based on the relative intersection of confidence interval rule and a robust median estimator. They give larger PSNR-s than competitive methods for different noise distributions. They offer better edge preservation and are less sensitive to outliers in the noisy image.

ACKNOWLEDGMENT

This work has been supported by the European Community Seventh Framework Programme under grant No. 285939 (ACROSS).

TABLE I. PSNR FOR 30 REALIZATIONS OF THE TEST IMAGE AND THREE DIFFERENT NOISE DISTRIBUTIONS: GAUSSIAN, LAPLACIAN AND BINOMIAL.

	Gaussian noise, dB	**Laplacian noise, dB**	**Binomial noise, dB**
noisy-image	28.1372	28.1263	27.7333
ICI, fixed weight	19.5834	19.5659	19.7396
ICI, variable weight	19.5706	19.5530	19.7269
MICI, fixed weight	28.1511	28.1373	27.7886
MICI, variable weight	28.1523	28.1405	27.7762
RICI, fixed weight	40.8962	38.9303	36.3624
RICI, variable weight	40.7430	39.0041	36.2947
MRICI, fixed weight	**42.1992**	**40.1020**	**42.6739**
MRICI, variable weight	**41.8532**	**40.1671**	**42.3026**
anisotropic LPA-ICI	39.9478	37.3952	35.5632
Haar wavelet	40.4542	39.7961	35.9131

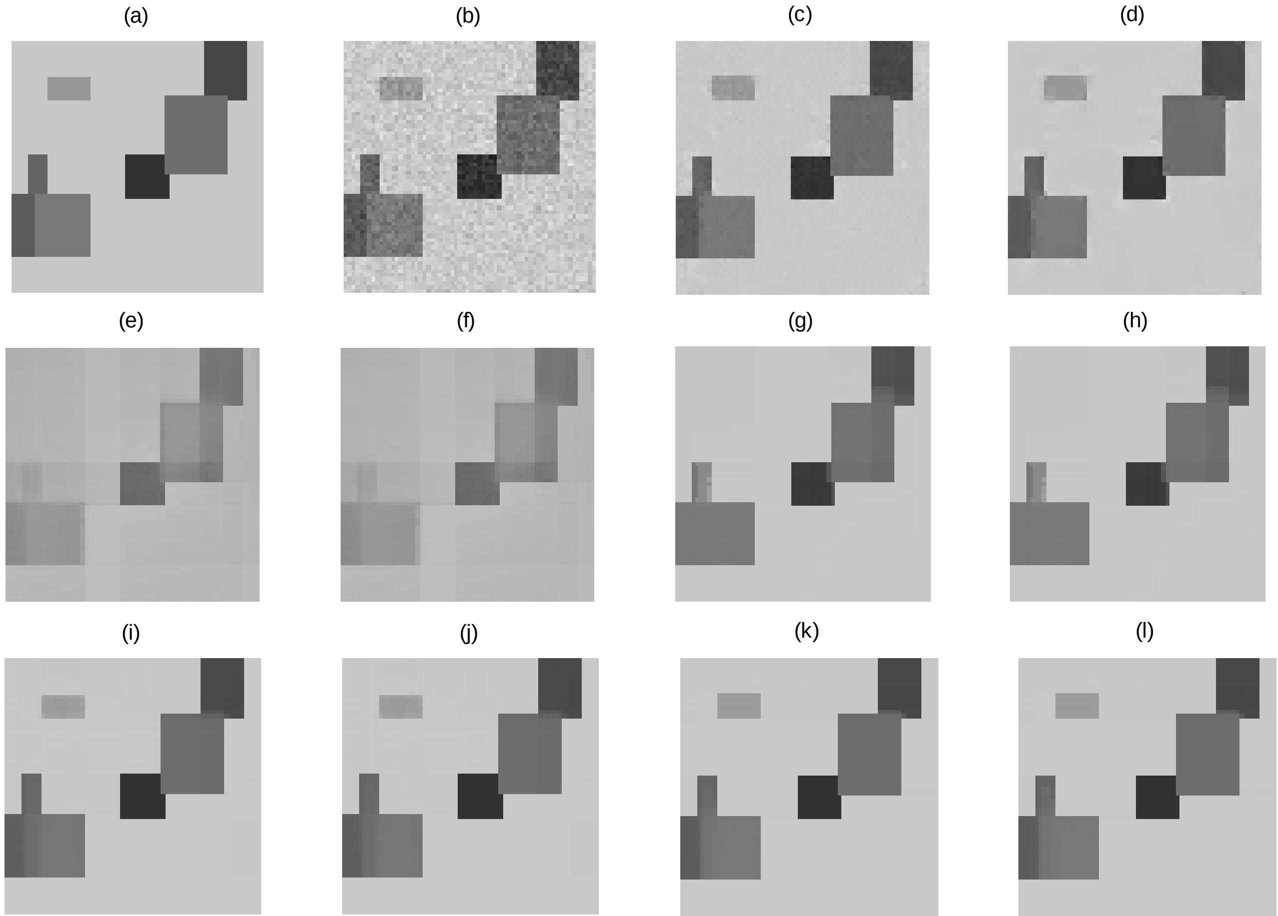

Fig. 1. (a) Test noise free image. (b) Noisy image with zero mean Gaussian noise $\sigma_w = 10$. (c) Anisotropic LPA-ICI denoised image with $\Gamma = 1.05$. (d) Undecimated Haar wavelet denoised image with hard threshold $3.5\sigma_w$ and 4 decomposition levels. (e) Mean ICI ($\Gamma = 4.4$) with fixed weights denoised image. (f) Mean ICI ($\Gamma = 4.4$) with variable weights denoised image. (g) Median ICI ($\Gamma = 4.4$) with fixed weights denoised image. (h) Median ICI ($\Gamma = 4.4$) with variable weights denoised image. (i) Mean RICI ($\Gamma = 4.4, r_c = 0.85$) with fixed weights denoised image. (j) Mean RICI ($\Gamma = 4.4, r_c = 0.85$) with variable weights denoised image. (k) Median RICI ($\Gamma = 4.4, r_c = 0.85$) with fixed weights denoised image. (l) Median RICI ($\Gamma = 4.4, r_c = 0.85$) with variable weights denoised image.

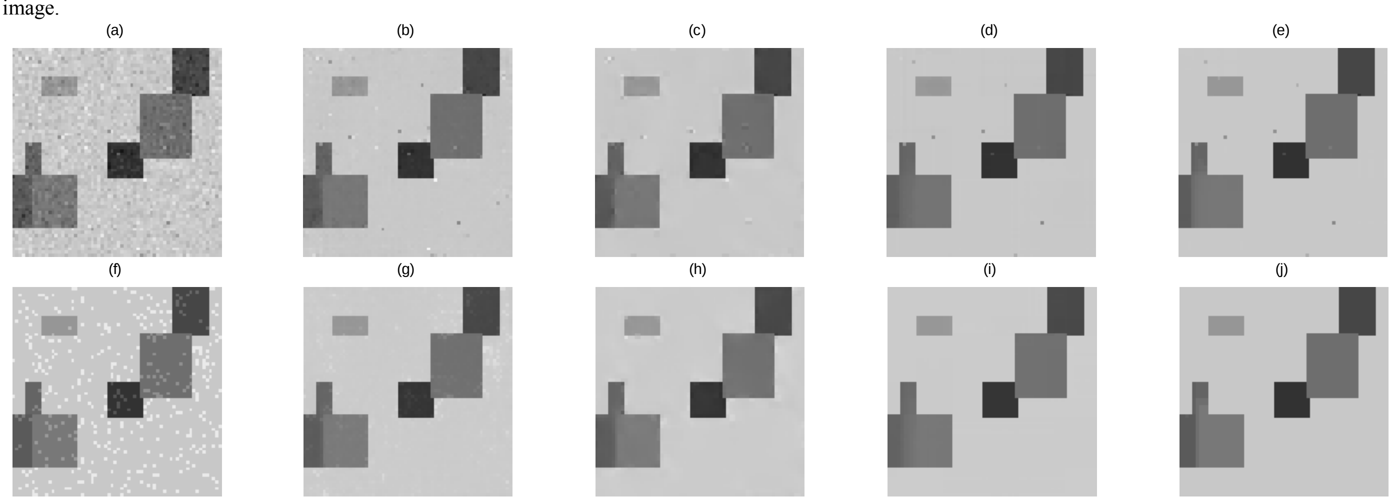

Fig. 2. (a) Image with added Laplacian noise $\sigma_w = 10$. (b) Anisotropic LPA-ICI denoised image with $\Gamma = 1.05$. (c) Undecimated Haar wavelet denoised image with hard threshold $3.5\sigma_w$ and 4 decomposition levels. (d) Mean RICI ($\Gamma = 4.4, r_c = 0.85$) with fixed weights denoised image. (e) Median RICI ($\Gamma = 4.4, r_c = 0.85$) with fixed weights denoised image. (f) Image with added binomial noise $\sigma_w = 10$. (g) Anisotropic LPA-ICI denoised image with $\Gamma = 1.05$. (h) Undecimated Haar wavelet denoised image with hard threshold $3.5\sigma_w$ and 4 decomposition levels. (i) Mean RICI ($\Gamma = 4.4, r_c = 0.85$) with fixed weights denoised image. (j) Median RICI ($\Gamma = 4.4, r_c = 0.85$) with fixed weights denoised image.

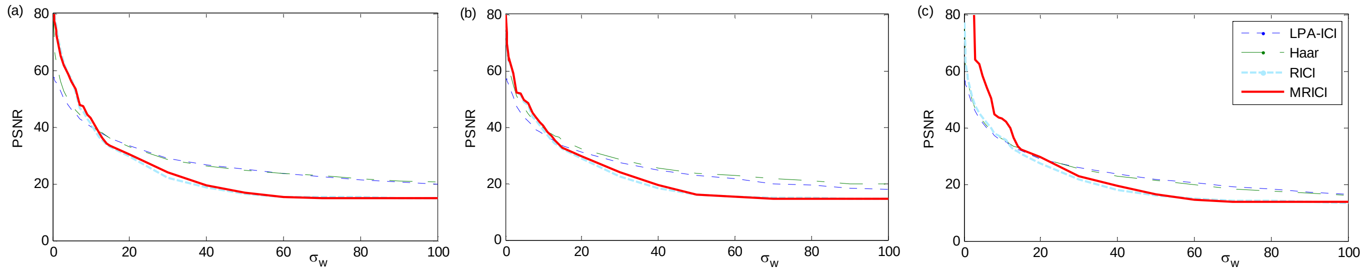

Fig. 3. PSNR as a function of σ_w for different denoising methods and different noise distributions: (a) Gaussian noise, (b) Laplacian noise and (c) binomial noise.

References

[1] R. Puetter, T. Gosnell, and A. Yahil, "Digital image reconstruction: deblurring and denoising," *Annual review of astronomy and astrophysics*, vol. 43, pp. 139–194, 2005.

[2] G. Cristobaly, M. Chagoyenz, B. Escalante-Ramirezx, and J. R. Lopez, "Wavelet-based denoising methods. a comparative study with applications in microscopy," in *Proc. SPIE's 1996 International symposium on optical science, engineering and instrumentation*, 1996.

[3] A. Buades, B. Coll, and J.-M. Morel, "A review of image denoising algorithms, with a new one," *SIAM Journal on multiscale modeling and simulation: A SIAM interdisciplinary journal*, vol. 4, no. 2, pp. 490–530, 2005.

[4] M. Tomić, S. Lončarić, and D. Seršić, "Adaptive spatio-temporal denoising of fluoroscopic X-ray sequences," *Biomedical signal processing and control*, vol. 7, no. 2, pp. 173–179, 2011.

[5] N. Wiener, *Extrapolation, interpolation, and smoothing of stationary time series*. New York: Wiley, 1949.

[6] J. Portilla, V. Strela, M. J. Wainwright, and E. P. Simoncelli, "Image denoising using gaussian scale mixtures in the wavelet domain," tech. rep., Courant institute of mathematical sciences, New York University, 2002.

[7] M. Vrankić and D. Seršić, "Image denoising based on adaptive QUINCUNX wavelets," in *IEEE 6th Workshop on MSP, Omnipress, Italy*, pp. 251–254, 2004.

[8] A. Sović and D. Seršić, "Adaptive wavelet image decomposition using LAD criterion," in *Proc. of the Eusipco, Spain*, pp. 594–598, 2011.

[9] A. Foi, V. Katkovnik, and K. Egiazarian, "Pointwise shape-adaptive DCT for high-quality denoising and deblocking of grayscale and color images," *IEEE Transactions on image processing*, vol. 16, no. 5, pp. 1395–1411, 2007.

[10] K. Dabov, A. Foi, V. Katkovnik, and K. Egiazarian, "Image denoising by sparse 3D transform-domain collaborative filtering," *IEEE Transactions on image processing*, vol. 16, no. 8, pp. 2080–2095, 2007.

[11] V. Katkovnik, K. Egiazarian, and J. Astola, "Adaptive window size image de-noising based on intersection of confidence intervals ICI rule," *Journal of mathematical imaging and vision*, vol. 16, no. 3, pp. 223–235, 2002.

[12] V. Katkovnik, "A new method for varying adaptive bandwidth selection," *IEEE Transaction on signal processing*, vol. 47, pp. 2567–2571, 1999.

[13] J. Lerga, M. Vrankić, and V. Sučić, "A signal denoising method based on the improved ICI rule," *Signal processing letters, IEEE*, vol. 15, pp. 601–604, 2008.

[14] J. Lerga, V. Sučić, and D. Seršić, "Performance analysis of the LPA-RICI denoising method," in *6th International symposium on image and signal processing and analysis ISPA Salzburg, Austria*, 2009.

[15] D. Seršić and A. Sović, "A robust improvement of the ICI rule for signal denoising," in *7th International symposium on image and signal processing and analysis*, pp. 26–31, 2011.

[16] J. Lerga, V. Sučić, and M. Vrankić, "Separable image denoising based on the relative intersection of confidence intervals rule," *Informatica*, vol. 22, no. 3, pp. 383–394, 2011.

[17] A. Foi, V. Katkovnik, K. Egiazarian, and J. Astola, "A novel anisotropic local polynomial estimator based on directional multiscale optimizations," in *6th IMA International conference mathematics in signal processing, Cirencester, U.K*, pp. 79–82, 2004.